Light bullets in the spatiotemporal nonlinear Schrödinger equation with a variable negative diffraction coefficient

Wei-Ping Zhong,[1,*] Milivoj Belić,[2,3] Gaetano Assanto,[4] Boris A. Malomed,[5,6] and Tingwen Huang[2]

[1]*Department of Electronic and Information Engineering, Shunde Polytechnic, Guangdong Province, Shunde 528300, China*
[2]*Texas A & M University at Qatar, 23874 Doha, Qatar*
[3]*Institute of Physics, University of Belgrade, P. O. Box 68, 11001 Belgrade, Serbia*
[4]*NooEL, Nonlinear Optics and OptoElectronics Lab, University of Rome "Roma Tre," I-00146 Rome, Italy*
[5]*Department of Physical Electronics, School of Electrical Engineering, Faculty of Engineering, Tel Aviv University, Tel Aviv 69978, Israel*
[6]*ICFO-Institut de Ciencies Fotoniques, Mediterranean Technology Park, E-08860 Castelldefels (Barcelona), Spain*[†]

We report approximate analytical solutions to the (3+1)-dimensional spatiotemporal nonlinear Schrödinger equation, with the uniform self-focusing nonlinearity and a variable *negative* radial diffraction coefficient, in the form of three-dimensional solitons. The model may be realized in artificial optical media, such as left-handed materials and photonic crystals, with the anomalous sign of the group-velocity dispersion (GVD). The same setting may be realized through the interplay of the self-defocusing nonlinearity, normal GVD, and positive variable diffraction. The Hartree approximation is utilized to achieve a suitable separation of variables in the model. Then, an inverse procedure is introduced, with the aim to select a suitable profile of the modulated diffraction coefficient supporting desirable soliton solutions (such as dromions, single- and multilayer rings, and multisoliton clusters). The validity of the analytical approximation and stability of the solutions is tested by means of direct simulations.

PACS number(s): 42.65.Tg, 05.45.Yv

I. INTRODUCTION

Light bullets, or optical spatiotemporal solitons [1], in which both the diffraction and group-velocity dispersion (GVD) are balanced by the nonlinearity, are challenging objects in nonlinear optics [2]. In addition to their fundamental significance as particle-like waves, light bullets can find application in long and short-distance communications, all-optical switching, and digital computing, among others [3]. Solitons in Kerr-type self-focusing media are governed by the cubic nonlinear Schrödinger (NLS) equation, and they are known to be unstable in two and three dimensions (2D and 3D) in homogeneous media, because of the collapse of the wave function. Various schemes to arrest the collapse were proposed, such as the use of weaker saturable [4,5] or quadratic nonlinearities [6–8], the application of the nonlinearity and/or GVD management [9], and the use of tandem structures, which are composed of periodically alternating linear dispersive and nonlinear layers [10].

Higher-dimensional NLS equations admit a broader variety of self-trapping scenarios than their 1D counterparts—in particular, "accessible" light bullets [11] and spatiotemporal bullet trains [12] in nonlocal 3D nematic liquid-crystal systems. However, the study of the multidimensional solitons is impeded by the lack of the corresponding integrable systems.

In this paper we find light-bullet solutions in the framework of the (3+1)D NLS equation with a negative variable diffraction coefficient, which depends on the transverse radial coordinate, while the negative GVD and self-focusing nonlinearity are uniform. The same equation, in its complex conjugate form, describes a medium with the positive variable diffraction coefficient, combined with the uniform normal GVD and self-defocusing cubic nonlinearity. Various optical media which admit the nonuniform diffraction, including that with the inverted (negative) sign, are available, such as photonic crystals [13]. The opposite relative sign of the diffraction and cubic nonlinearity precludes the collapse in the present case [14], although the same feature poses a question regarding how, in principle, self-trapped modes may be supported in this case, as the existence of bright spatial solitons requires, usually, identical signs of the nonlinearity and diffraction. As we argue below, comparison with recent works [15] suggests that this counterintuitive result of the interplay of the nonlinearity and diffraction is possible because, essentially, the nonzero diffraction is bounded (in the present model) to a finite area; see Figs. 1(d), 2(d), 3(d), and 4(d) below. On the other hand, the use of the variable transverse diffraction coefficient makes the model and solitary waves found in it akin to the nonautonomous solitons which may be supported by diverse variants of the "management" techniques [16,17]. In particular, the stabilization of 3D solitons by a variant of the management based on out-of-phase sign-changing oscillations of the nonlinearity and strength of the external trap (i.e., alternation of waveguiding and anti-waveguiding segments of the trap, which is a known setting that can support spatial solitons [18]) was recently elaborated in Ref. [19].

To construct the localized modes, we employ the Hartree approximation, which yields a factorized solution with separated variables. We then express the solution in terms of two arbitrary (but appropriately chosen) functions, which imply a rich structure of the beam field. In particular,

*zhongwp6@126.com
†Sabbatical address

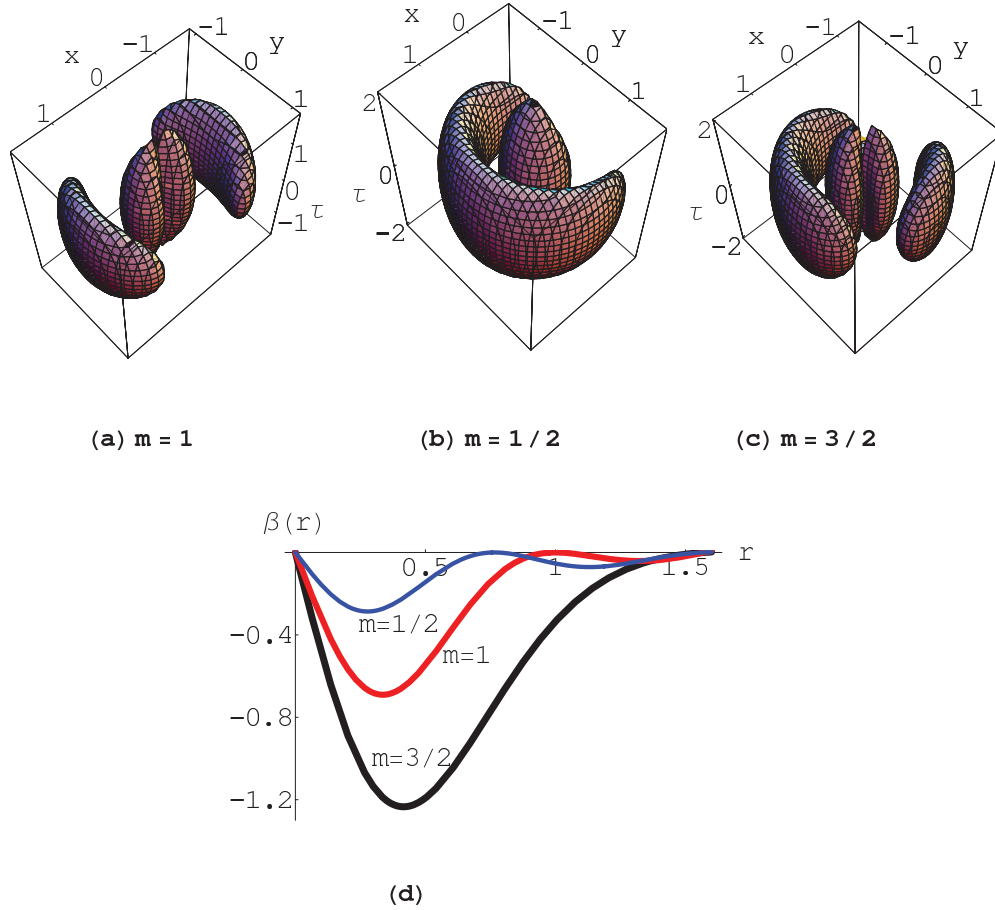**(a) m = 1**   **(b) m = 1 / 2**   **(c) m = 3 / 2**

(d)

FIG. 1. (Color online) Typical localized light-bullet patterns (the top row), and the corresponding diffraction function $\beta(r)$ (the bottom row). Intensity isosurfaces of light bullets are displayed for different values of the topological charge, m. Other parameters: $a_0 = 16$, $q = 0$.

one can find localized excitations that include "dromions," ring solitons, soliton clusters, etc., which are all derived from the general 3D light bullet solution. The freedom in the choice of the functions comprising the solution makes it feasible to formulate an *inverse* problem: First, define appropriate expressions for the two arbitrary functions, which describe the desired localized mode, and then find the corresponding diffraction coefficient, which produces such a solution. Following this route, we construct some interesting approximate analytical solutions for the localized structures. The careful choice of the two arbitrary functions may lead to realistic models of dispersion and diffraction in various media. We find that the appropriate diffraction coefficients, leading to desirable localized solutions, are *negative* and oscillating. Materials displaying such effective diffraction include left-handed materials, nematic liquid crystals, and photonic crystals [13]. The stability of the so-constructed localized solutions is verified by direct simulations.

The paper is structured as follows. In Sec. II the solution method is introduced. Localized solutions are presented in Sec. III, and results of simulations are displayed in Sec. IV. Section V concludes the paper.

II. THE SOLUTION METHOD

We begin the analysis from the scaled (3+1)D spatiotemporal nonlinear Schrödinger equation [2], [9], [13]:

$$i\frac{\partial u}{\partial z} + \frac{1}{2}\left[\beta(r)\nabla_\perp^2 u + \frac{\partial^2 u}{\partial \tau^2}\right] + |u|^2 u = 0, \qquad (1)$$

which governs the propagation of a slowly varying field envelope u along coordinate z in the self-focusing Kerr optical medium, characterized by the variable diffraction coefficient $\beta(r)$, while the coefficient of the anomalous GVD is scaled to be 1. Here $\nabla_\perp^2$ is the transverse 2D Laplacian, τ is the retarded time in the reference frame moving with the pulse, and $r = \sqrt{x^2 + y^2}$ is the transverse radial coordinate. Although the form of Eq. (1) seems non-Lagrangian, it can be made derivable from the Lagrangian if the equation is divided by coefficient $\beta(r)$.

Dealing with the model in the form of Eq. (1), we will only consider the one with the negative diffraction, $\beta < 0$. However, applying the complex conjugation to Eq. (1), and making use of the complex-conjugate field variable, u^*, it is obvious that Eq. (1) is tantamount to a more realistic physical

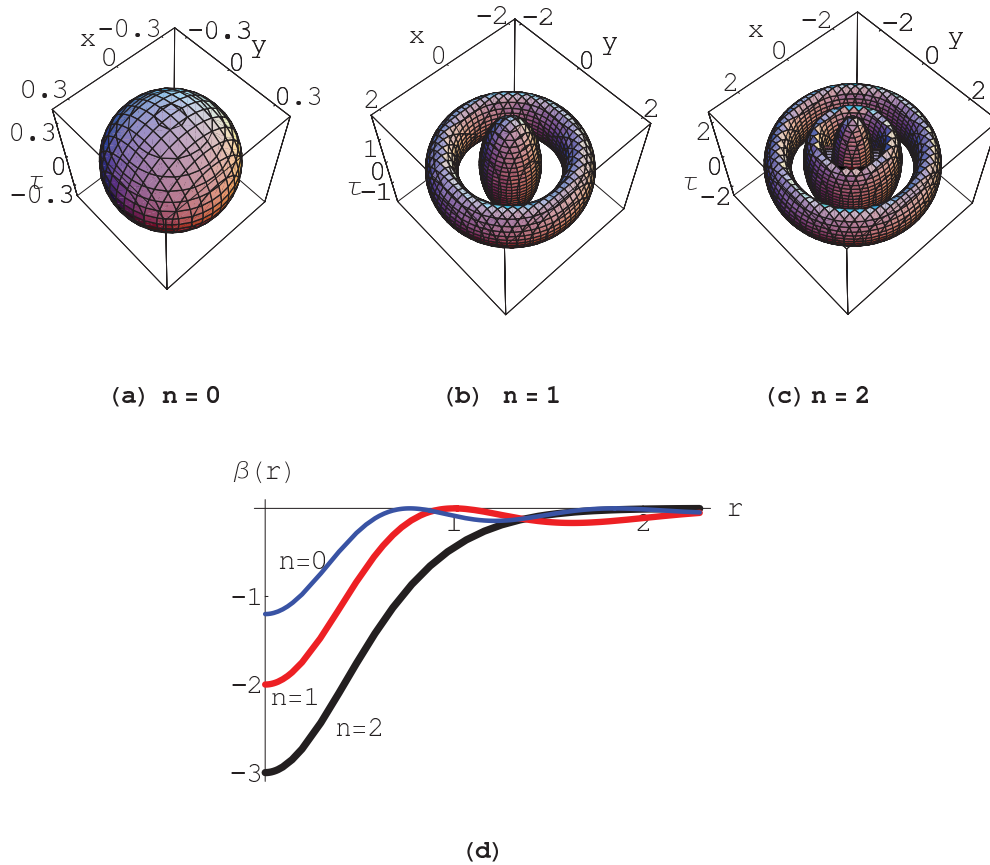**(a) n = 0**   **(b) n = 1**   **(c) n = 2**

(d)

FIG. 2. (Color online) [(a)–(c)] Isosurface profiles of the multidromion modes for $m = 0$ and $n = 0,1,2$, respectively. (d) The corresponding diffraction functions.

model, combining the positive diffraction, self-defocusing nonlinearity, and normal GVD.

Using polar coordinates (r,φ), we search for solutions to Eq. (1) that separate the variables:

$$u(z,r,\phi,\tau) = \Phi(\varphi)\, U(z,r,\tau), \qquad (2)$$

with the azimuthal part

$$\Phi(\varphi) = \cos(m\varphi) + iq\sin(m\varphi), \qquad (3)$$

where m is a non-negative real topological charge. Under certain circumstances, the effective topological charge may be fractional, allowing the possibility of *fractional* angular momentum; such a possibility has recently been discussed theoretically [20,21] and demonstrated experimentally [22–24].

Parameter $q \in [0,1]$ in Eq. (3) determines the depth of the azimuthal modulation. With this form of the azimuthal function, the nonlinearity retains the φ dependence in $|u|^2$. Still, we will employ this form of function $\Phi(\varphi)$ to derive an equation for U in which the influence of φ is *averaged* out, in the spirit of the mean-field approximation. This approximation is relevant for the weak nonlinearity and for large q, close enough to 1.

Substituting expression (2) into Eq. (1) and integrating over φ from 0 to 2π, we obtain the following *averaged* equation,

for integer or half-integer m:

$$i\frac{\partial U}{\partial z} + \frac{1}{2}\beta(r)\left(\frac{\partial^2 U}{\partial r^2} + \frac{1}{r}\frac{\partial U}{\partial r} - \frac{m^2 U}{r^2}\right) + \frac{1}{2}\frac{\partial^2 U}{\partial \tau^2}$$
$$+ \frac{1}{2}(1 + q^2)|U|^2 U = 0. \qquad (4)$$

In the general case, one can represent complex field $U(z,r,\tau)$ in terms of amplitude A and phase B:

$$U(z,r,\tau) = A(r,\tau)\, e^{iB(r,\tau) + ik_0 z}, \qquad (5)$$

where k_0 is the propagation constant. The substitution of this expression into Eq. (4) and separation of the real and imaginary parts leads to coupled equations for A and B,

$$-k_0 A + \frac{1}{2}\beta\left[\frac{\partial^2 A}{\partial r^2} - A\left(\frac{\partial B}{\partial r}\right)^2 + \frac{1}{r}\frac{\partial A}{\partial r} - \frac{m^2 A}{r^2}\right]$$
$$+ \frac{1}{2}\left[\frac{\partial^2 A}{\partial \tau^2} - A\left(\frac{\partial B}{\partial \tau}\right)^2\right] + \frac{1}{2}(1 + q^2)A^3 = 0, \qquad (6a)$$

$$\beta\left[2\frac{\partial A}{\partial r}\frac{\partial B}{\partial r} + A\frac{\partial^2 B}{\partial r^2} + \frac{1}{r}\frac{\partial B}{\partial r}A\right] + 2\frac{\partial A}{\partial \tau}\frac{\partial B}{\partial \tau} + A\frac{\partial^2 B}{\partial \tau^2} = 0. \qquad (6b)$$

In general, this system of equations is difficult to treat analytically. One approach is to assume specific forms for
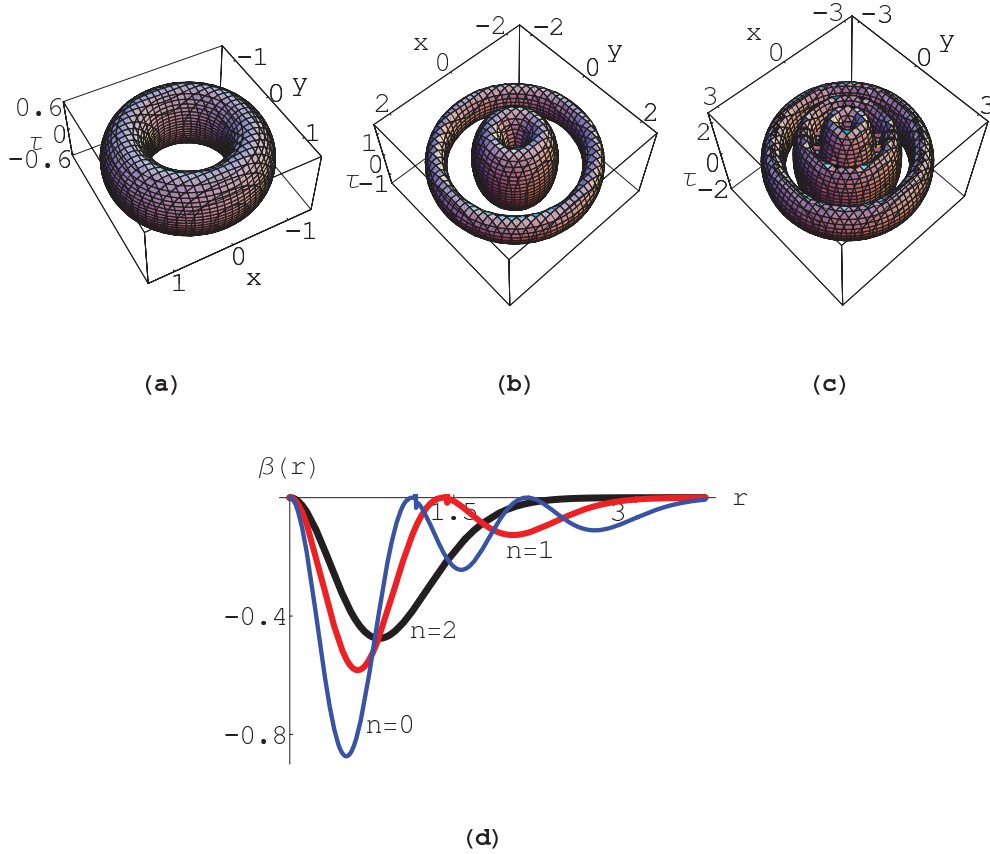
FIG. 3. (Color online) [(a)–(c)] Intensity distributions in the ring-shaped modes, for $q = 1, m = 1$ and $n = 0, 1, 2$, from left to right. (d) The corresponding dispersion functions.

amplitude $A(r, \tau)$ and the phase $B(r, \tau)$ and then analyze the resulting equations for the presumed solutions. Another possibility is to assume a specific form for B in terms of A, which formally solves Eq. (6b), and then deal with the equation for A. In this work, we consider the simplest possibility, when B is a constant; hence Eq. (6b) drops out, and Eq. (6a) becomes

$$\frac{\partial^2 A}{\partial \tau^2} + \beta \left[\frac{\partial^2 A}{\partial r^2} + \frac{1}{r} \frac{\partial A}{\partial r} - \frac{m^2}{r^2} A \right] + (1 + q^2) A^3 - 2k_0 A = 0. \tag{7}$$

We treat Eq. (7) by means of the Hartree approximation [25–28], which is based on the product ansatz,

$$A(r, \tau) = R(r) T(\tau) \tag{8}$$

that, again, separates the variables. Substituting this into Eq. (7), we arrive at the equation

$$R \frac{\partial^2 T}{\partial \tau^2} + (1 + q^2) R^3 T^3 + \beta \left[\frac{\partial^2 R}{\partial r^2} + \frac{1}{r} \frac{\partial R}{\partial r} - \frac{m^2}{r^2} R \right] T - 2k_0 R T = 0. \tag{9}$$

Similarly to what we encountered above, the nonlinearity does not allow the rigorous separation of the variables. We proceed, as before, by deriving the averaged equations for R and T, following the Hartree approximation. Multiplying

Eq. (9) by R, integrating it over r from 0 to ∞, and dividing by $\int_0^\infty R^2 dr$, leads to the following equation for $T(\tau)$:

$$\frac{\partial^2 T}{\partial \tau^2} + \frac{1}{2} (1 + q^2) T^3 - T = 0. \tag{10}$$

Here, the localization is assumed, $R(r \to \infty) = 0$, and $k_0 = \frac{1}{2}$ is fixed by scaling. An obvious relevant solution of Eq. (10), to be utilized here, is the bright solitary wave, $T(\tau) = \frac{2}{\sqrt{1+q^2}} \operatorname{sech}(\tau)$. Similarly, if Eq. (9) is multiplied by T, integrated from $-\infty$ to $+\infty$, and divided by $\int_{-\infty}^\infty T(\tau)^2 d\tau$, one obtains

$$3\beta \left(r^2 \frac{\partial^2 R}{\partial r^2} + r \frac{\partial R}{\partial r} - m^2 R \right) + 8r^2 R^3 - 4r^2 R = 0. \tag{11}$$

The treatment of Eq. (11) is more difficult. Using the fact that the function $\beta(r)$ was not specified yet, we *invert* the procedure: Rather than treating Eq. (11) as an equation for R with given β, we assume that it is an equation for β with given R. Thus, with R given in a certain form, β is determined following a procedure which may be facilitated by the use of the Hirota binary operator [29,30], $D_r(g(r) f(r)) = \left(\frac{\partial}{\partial r} - \frac{\partial}{\partial r'} \right) g(r) f(r') \big|_{r=r'}$. To this end, we assume that amplitude R can be presented as a quotient, $R(r) = \frac{g}{f}$, of two arbitrary nonzero real functions $g(r)$ and

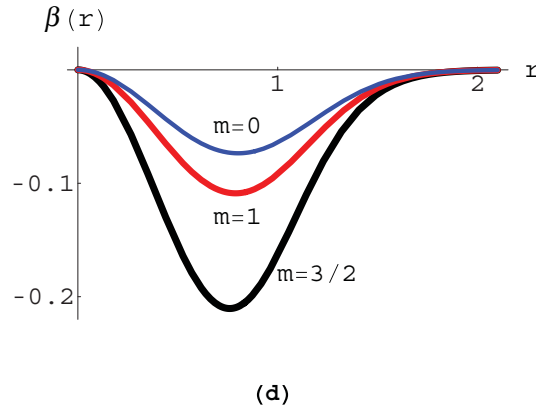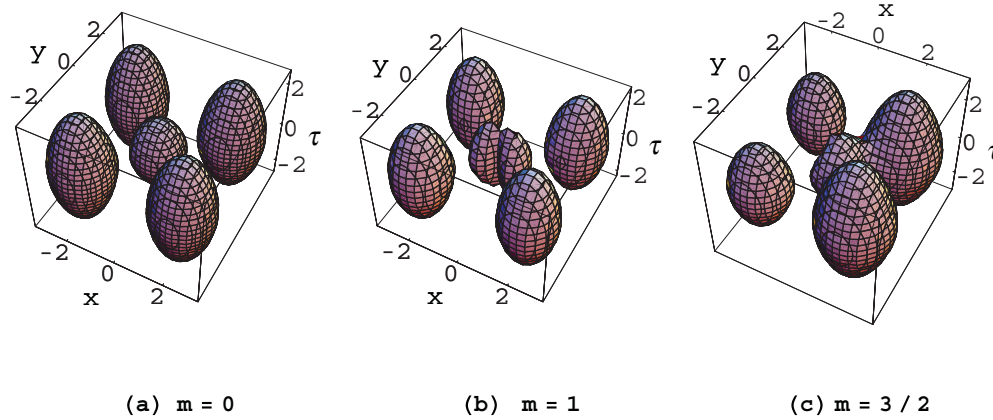**(a) m = 0**   **(b) m = 1**   **(c) m = 3 / 2**

(d)

FIG. 4. (Color online) [(a)–(c)] Bound state in the form of clustered Gaussians, and (d) the corresponding diffraction functions, for $m = 0,1,3/2$. The corresponding functions g and f and other parameters are defined in the text.

$f(r)$. Then, Eq. (11) yields an expression for the diffraction coefficient $\beta(r)$ in terms of the Hirota's bilinear form:

$$\beta(r) = \frac{4gr^2(f^2 - 2g^2)}{3\left\{r^2\left[fD_r^2(gf) - gD_r^2(ff)\right] + rfD_r(gf) - m^2gf^2\right\}}. \tag{12}$$

Hence, by an appropriate choice of functions f and g, leading to a localized spatial part R of the light-bullet solution, one can determine the diffraction coefficient β for which such solutions are allowed.

At this point it is relevant to recall the full form of the approximate light-bullet solution of Eq. (1), as per substitutions (2), (3), (5), and (8):

$$u(z,r,\varphi,\tau) = \frac{2(\cos m\varphi + iq\sin m\varphi)}{\sqrt{1+q^2}}\frac{g}{f}\operatorname{sech}(\tau)\,e^{iB + \frac{i}{2}z}, \tag{13}$$

where $B = \text{const}$ and $k_0 = \frac{1}{2}$, as fixed above. Selecting relevant arbitrary functions $g(r)$ and $f(r)$ in Eq. (13), one may construct various localized structures in the models with the diffraction coefficient defined by Eq. (12).

A similar inverse problem, i.e., constructing a potential function which would produce a desired solution to the equation, was presented in Ref. [31] for 1D and 2D

Gross-Pitaevskii equations. Crucial to this procedure is the proper choice of boundary conditions, in particular those for localized solutions. Below we present relevant examples of so-generated solutions.

III. LOCALIZED MODES

While the choice of functions f and g is arbitrary, care must be taken to produce physically relevant localized solutions. Initially, we choose these functions in Eq. (13) as $g = \sin(r^2 - a_0)$ and $f = \exp(r^2/2)$, where a_0 is an arbitrary constant. Such a choice leads to the localized excitations resembling "dromions" [32–34], which decay exponentially in all directions, as shown in Figs. 1(a)–1(c) for $a_0 = 16$. For given g and f, the corresponding $\beta(r)$ is calculated from Eq. (12). The graphs of $\beta(r)$ for different m are shown in Fig. 1(d). It is seen that the diffraction coefficient vanishes at $r = 0$, being *negative* at $r > 0$. In the limit
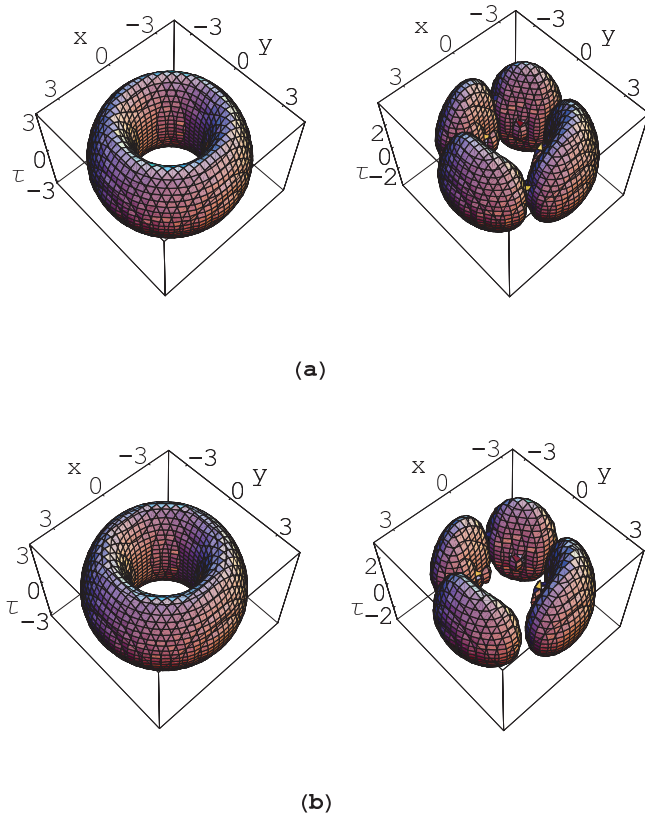
(a)

(b)

FIG. 5. (Color online) Comparison of the approximate solutions with their numerical counterparts for $q = 1$ (left column) and $q = 0$ (right column). (a) The intensity distribution as predicted by the analytical expression (13). (b) The respective numerical solution of Eq. (1), after propagation distance $z = 50$. The corresponding functions g and f and the parameters are defined in the text.

of $q = 0$ and for $m \neq 0$, the localized modes feature two radial layers. The modes with integer m are built of $4m$ bright spots, while half-integer m gives rise to asymmetric localized patterns, structured along the azimuthal coordinate and featuring $2m + 1$ bright spots.

It is commonly known that bright spatial solitons exist under the action of the diffraction and cubic nonlinearity with identical signs, while, in the present case, $\beta(r) < 0$ has the sign *opposite* to that of the cubic term in Eq. (11). Actually, solitons may exist in this setting due to the fact that nonzero values of $\beta(r)$ are confined to a finite region, as seen in Fig. 1(d). To better understand this feature, we refer to recent works [15], which are dealing with the normal diffraction and *self-defocusing* cubic term, the coefficient in front of which quickly diverges at $|x| \to \infty$:

$$i\frac{\partial u}{\partial z} + \frac{1}{2}\frac{\partial^2 u}{\partial x^2} - e^{\frac{1}{2}x^2}|u|^2 u = 0. \tag{14}$$

In spite of the "wrong" relative sign of the diffraction and nonlinearity, this equation gives rise to stable bright solitons, including, for instance, an *exact* solution for the dipole soliton, $u(z,x) = \frac{x}{\sqrt{2}}\exp[-\frac{1}{2}(3iz + x^2)]$. Now, dividing Eq. (14) by $\exp(x^2/2)$, and taking into regard that function $\exp(-x^2/2)$, practically, differs from zero in a finite region, we conclude that the stationary version of the so-obtained equation is quite

similar to those considered above with the negative diffraction coefficient confined to the finite region. This comparison helps to understand the reason for the existence of bright solitons in the present model.

Examples of multiple dromion-like [32,33], [34] and multiple-ring [35] axially symmetric modes are obtained with other choices of functions g and f. For instance, the light bullets obtained with

$$g = r^m L_n^m(r^2), \quad f = e^{\frac{1}{2}r^2}, \tag{15}$$

where L_n^m are the generalized Laguerre polynomials and n is an integer, are displayed in Figs. 2 and 3. Parameters q, m, and n control the shape of these modes as per Eq. (13), for the corresponding $\beta(r)$ functions, which are calculated from Eq. (12) and displayed in Figs. 2(d) and 3(d). When $m = 0$ ($q = 1$), the multi-dromion (multi-ring) solutions can be obtained for different values of n. For $n = 0$, a single-dromion solution of the instanton type is found, see Fig. 2(a), and multidromions are obtained for $n \geqslant 1$. Two- and three-layer dromions are plotted in Figs. 2(b) and 2(c). The multidromion modes feature $n + 1$ layers for $n \geqslant 1$.

Modes shaped as thin rings are obtained with $m = 1$ and $q = 1$. Examples of the rings are shown in Fig. 3. For $n = 0$, the single-ring mode is shown in the left panel of Fig. 3. For integer $n \geqslant 1$, these light bullets feature $n + 1$ layers; see Fig. 3(b) and 3(c).

The corresponding diffraction coefficient is presented in Fig. 3(d) for $m = 1$ and different values of n. In this case, too, β is negative, being zero at the center. As mentioned, possible materials for the observation of such light bullets might be nematic liquid crystals (NLCs), photonic crystals, and left-handed materials. The self-focusing of the light beam in bulk NLC was reported in Ref. [36]. It is relevant to mention that the field-induced complex refractive index changes in nano-dispersed NLCs, exhibiting negative and positive refractive indices, are achieved at different values of the strength of the applied field and different anchoring conditions, over a broad spectral regime. Partially incoherent spatial solitons have been observed in undoped E7 NLC cells [37,38]. These incoherent solitons ("nematicons") were generated at milliwatt power levels in voltage-biased planar cells.

It is also possible to construct bound states of an arbitrary number of localized modes. For this purpose, we introduce f and g as Gaussian functions, $g = a_0 + \sum_{n=1}^{N} b_n e^{-(\vec{r}-\vec{r}_n)^2}$ and $f = d_0 + \sum_{j=1}^{J} c_j e^{-(\vec{r}-\vec{r}_j)^2}$, where $a_0(\neq 0)$, b_n, $d_0(\neq 0)$, c_j, $\vec{r}_n$, and $\vec{r}_j$ are arbitrary constants. The analytical solution given by Eq. (13) in this case, and the corresponding function $\beta(r)$ given by Eq. (12), can be easily written down. The number of localized modes in the bound state is controlled by N and J, and the amplitude and the location of each mode are determined by parameters a_0, b_n, d_0, c_j, and $\vec{r}_n, \vec{r}_j$, respectively. This type of clustered solutions, generated by Eq. (13), can generate sundry profiles. For example, choosing $N = 5$, $J = 1$, $a_0 = b_2 = b_3 = b_4 = b_5 = d_0 = c_1 = 1$, $b_1 = 2\sqrt{e}$ and $\vec{r}_1 = (0,0)$, $\vec{r}_2 = (2,2)$, $\vec{r}_3 = (-2,-2)$, $\vec{r}_4 = (2,-2)$, $\vec{r}_5 = (-2,2)$, we obtain the patterns shown in Fig. 4.

In Fig. 4(a), $m = 0$ gives rise to a complex built of five localized modes, with the one located at the center having a smaller amplitude than the other four. For $m = 1$, the pattern

is formed by six local modes, with two of them, that have the lower amplitude, set close to the center; see Fig. 4(b). Half-integer m gives rise to an asymmetric pattern; see Fig. 4(c). As seen in Fig. 4(d), the diffraction coefficient supporting the clustered patterns must again be negative.

IV. COMPARISON WITH DIRECT SIMULATIONS

The expression given by Eq. (13) is an approximate solution of Eq. (1). Therefore, it is necessary to verify the existence and stability of the so-predicted states by means of a direct numerical solution of Eq. (13), which was done with the help of the split-step beam propagation method [28,39] for the initial configuration taken as per Eq. (13) at $z = 0$,

$$u\left(0,r,\varphi,\tau\right) = \frac{2\left(\cos m\varphi + iq\sin m\varphi\right)}{\sqrt{1+q^2}} \frac{g}{f} \operatorname{sech}\left(\tau\right) e^{iB},$$

the same functions $g(r)$ and $f(r)$ as in Eq. (15), and the corresponding diffraction-coefficient function; see Eq. (12). Setting $m = 3/2$ and $n = 1$, the corresponding plot of the intensity distribution, $|u(z,r,\varphi,\tau)|^2$, as produced by the numerical solution, is compared to the respective approximate solution, given by Eq. (13), for $q = 0$ and $q = 1$. The numerical solution does not give to any visible instability, and good agreement with the approximate analytical solution is observed (see Fig. 5). Similar behavior was seen for other initial conditions.

V. CONCLUSIONS

In this work, we have studied localized modes in the (3+1)D spatiotemporal nonlinear Schrödinger equation with the self-focusing nonlinearity, anomalous GVD, and a variable negative diffraction coefficient, which is effectively confined to a finite region. The same model applies to the medium combining the positive diffraction, self-defocusing nonlinearity, and normal GVD. Using the Hirota's bilinear method and Hartree approximation, we have determined a variety of profiles of the modulated diffraction coefficient that can maintain light-bullet modes with different desired shapes. Specific features of the localized patterns supported by such engineered profiles of the diffraction coefficient were discussed. The existence of the spatially localized modes, despite the negative relative sign of the cubic nonlinearity and diffraction, was explained qualitatively, a key property being the fact that the diffraction coefficient differs from zero in a finite region. The validity of the analytical approximation was verified by direct simulations of the underlying NLS equation.

[1] Y. Silberberg, Opt. Lett. **15**, 1282 (1990).

[2] B. A. Malomed, D. Mihalache, F. Wise, and L. Torner, J. Opt. B **7**, R53 (2005).

[3] F. K. Abdullaev and V. V. Konotop (eds.), *Nonlinear Waves: Classical and Quantum Aspects* (Kluwer, Dordrecht, 2004).

[4] D. E. Edmundson and R. H. Enns, Opt. Lett. **17**, 586 (1992).

[5] W. P. Zhong, R. H. Xie, M. Belic, N. Petrovic, and G. Chen, Phys. Rev. A **78**, 023821 (2008).

[6] A. A. Kanashov and A. M. Rubenchik, Physica D **4**, 122 (1981).

[7] B. A. Malomed, P. Drummond, H. He, A. Berntson, D. Anderson, and M. Lisak, Phys. Rev. E **56**, 4725 (1997).

[8] V. N. Serkin and A. Hasegawa, Phys. Rev. Lett. **85**, 4502 (2000).

[9] M. Matuszewski, M. Trippenbach, B. A. Malomed, E. Infeld, and A. A. Skorupski, Phys. Rev. E **70**, 016603 (2004); M. Matuszewski, E. Infeld, B. A. Malomed, and M. Trippenbach, Opt. Commun. **259**, 49 (2006).

[10] L. Torner, S. Carrasco, J. P. Torres, L.-C. Crasovan, and D. Mihalache, Opt. Commun. **199**, 277 (2001); L. Torner and Y. V. Kartashov, Opt. Lett. **34**, 1129 (2009).

[11] I. B. Burgess, M. Peccianti, G. Assanto, and R. Morandotti, Phys. Rev. Lett. **102**, 203903 (2009).

[12] M. Peccianti, I. B. Burgess, G. Assanto and R. Morandotti, Opt. Express **18**, 5934 (2010).

[13] Y. S. Kivshar, and G. P. Agrawal, *Optical Solitons: From Fibers to Photonic Crystals* (Academic Press, New York, 2003).

[14] C. Sulem and P. Sulem, *The Nonlinear Schrödinger Equation: Self-Focusing and Wave Collapse* (Springer-Verlag: Berlin, 2000).

[15] O. V. Borovkova, Y. V. Kartashov, B. A. Malomed, and L. Torner, Opt. Lett. **36**, 3088 (2011); O. V. Borovkova, Y. V. Kartashov, L. Torner, and B. A. Malomed, Bright Solitons from Defocusing Nonlinearities, Phys. Rev. E (in press).

[16] B. A. Malomed, *Soliton Management in Periodic Systems* (Springer, New York, 2006).

[17] V. N. Serkin, A. Hasegawa, and T. L. Belyaeva, J. Mod. Opt. **57**, 1456 (2010); Phys. Rev. A **81**, 23610 (2010).

[18] A. Kaplan, B. V. Gisin, and B. A. Malomed, J. Opt. Soc. Am. B **19**, 522 (2002).

[19] T. L. Belyaeva, V. N. Serkin, M. A. Aguero, C. Hernandez-Tenorio, and L. M. Kovachev, Laser Physics **21**, 258 (2011).

[20] M. V. Berry, J. Opt. A: Pure Appl. Opt. **6**, 259 (2004).

[21] I. V. Basistiy, V. A. Pas'ko, V. V. Slyusar, M. S. Soskin, and M. V. Vasnetsov, J. Opt. A: Pure Appl. Opt. **6**, S166 (2004).

[22] W. M. Lee, X. C. Yuan, and K. Dholakia, Opt. Commun. **239**, 129 (2004).

[23] J. Leach, E. Yao, and M. J. Padget, New J. Phys. **6**, 71 (2004).

[24] S. H. Tao, X. C. Yuan, J. Liu, X. Peng, and H. B. Niu, Opt. Express **13**, 7726 (2005).

[25] K. Hayata and M. Koshiba, Phys. Rev. Lett. **71**, 3275 (1993).

[26] K. Hayata and M. Koshiba, Phys. Rev. E **48**, 2312 (1993).

[27] N. K. Efremidis, K. Hizanidis, B. A. Malomed, and P. Di Trapani, Phys. Rev. Lett. **101**, 113901 (2008).

[28] W. P. Zhong, M. Belić, and T. W. Huang, Phys. Rev. A **82**, 033834 (2010).

[29] R. Hirota, Phys. Rev. Lett. **27**, 1192 (1971).

[30] W. P. Zhong and H. Luo, Chin. Phys. Lett. **17**, 577 (2000).

[31] B. A. Malomed and Y. A. Stepanyants, Chaos **20**, 013130 (2010).

[32] M. Boiti, J. J. Leon, M. Manna, and F. Pempinelli, Inverse Probl. **2**, 271 (1986).

[33] M. Boiti, J. J. Leon, and F. Pempinelli, Inverse Probl. **3**, 371 (1987).

[34] A. S. Fokas and P. M. Santini, Phys. Rev. Lett. **63**, 1329 (1989); A. Fokas and P. M. Santini, Physica D **44**, 99 (1990); J. Hietarinta and R. Hirota, Phys. Lett. A **145**, 237 (1990); J. Hietarinta, Phys. Lett. A **149**, 113 (1990).

[35] W. P. Zhong and M. Belic, Phys. Rev. A **79**, 023804 (2009).

[36] G. Pawlik, M. Jarema, W. Walasik, A. C. Mitus, and I. C. Khoo, J. Opt. Soc. Am. B **27**, 567 (2010).

[37] G. Assanto and M. Peccianti, IEEE J. Quantum Electron. **39**, 13 (2003).

[38] M. Peccianti and G. Assanto, Phys. Rev. E **65**, 035603(R) (2002).

[39] M. Belic, N. Petrovic, W. P. Zhong, R. H. Xie, and G. Chen, Phys. Rev. Lett. **101**, 123904 (2008).